Biotechnological Communication

Biosci. Biotech. Res. Comm. 10(1): 63-71 (2017)

BBRC Bioscience Biotechnology Research Communications

Development of 3D QSAR based pharmacophore model for neuraminidase in Influenza A Virus

Sudha Singh, Anvita Gupta Malhotra, Mohit Jha and Khushhali M. Pandey*

Department of Biological Science and Engineering Maulana Azad National Institute of Technology, Bhopal (India)

ABSTRACT

A number of new advances in computer - aided drug designing have reduced the effective cost and time involved in drug discovery. However, the quest for more effective compounds often faces stiff challenge due to increased drug resistance. Pharmacophore modeling has emerged as a method with a lot of potential and is increasingly used for designing new molecules by using available knowledge of activity of compounds. 3D Quantitative Structure - Activity Relationship (QSAR) based pharmacophore modeling is a reliable method for developing new chemical moieties. Influenza A virus results in acute respiratory infection with serious consequences for the elderly and high – risk patients. Neuraminidase inhibitors are the well - known drugs that are frequently used against influenza virus. The current work has focused on developing a 3D QSAR based pharmacophore model for neuraminidase enzyme by using a dataset of known inhibitors. The best quantitative pharmacophore model selected was made of one hydrogen bond acceptor, one hydrogen bond donor and hydrophobic aliphatic features with high correlation value of 0. 917. Pharmacophore model was cross - validated by Fischer randomization and leave - one - out method to check the reliability of model. The findings can prove out to be quite helpful in screening new molecules against neuraminidase.

KEY WORDS: NEURAMINIDASE, DISCOVERY STUDIO, 3D - QSAR, PHARMACOPHORE, COMPUTER – AIDED DRUG DESIGN

INTRODUCTION

Influenza virus is a member of Orthomyxoviridae family of viruses. Based on differences in the nucleoprotein (NP) and matrix (M1) protein, this virus is classified into three major categories - A, B and C. Influenza A, known for the infection of mammalian species, is divided into 18 HA subtypes (H1 - H17) and 11 NA (N1 - N9). This division is based on serological reactivates of surface proteins, hemagglutinin (HA) and neuraminidase (NA) (Ferguson et al., 2015, Ducatez et al., 2015). Various types of influenza viruses have significant difference in

ARTICLE INFORMATION:

**Corresponding Author: menaria.khushhali@gmail.com*

Received 27th Nov, 2016
Accepted after revision 21st Feb, 2017
BBRC Print ISSN: 0974-6455
Online ISSN: 2321-4007 CODEN: USA BBRCBA
Thomson Reuters ISI ESC and Crossref Indexed Journal
NAAS Journal Score 2017: 4.31 Cosmos IF : 4.006

Online Contents Available at: http//www.bbrc.in/

their host range and pathogenicity. They infect a variety of animals including pigs, horses, whales, dogs, bats and birds (Nayak et al., 2010, Rajao and Vincent, 2015).

Infection caused by Influenza virus, commonly known as flu, is responsible for acute respiratory infection, with significant morbidity in the population and mortality in the elderly and high–risk patients. It is also a prominent cause of disability and death and is therefore a serious public health issue (Kobasa et al., 2004). One of the main limitations in new drug discovery is drug resistance in mutant strains (Renzette et al., 2014). M2 protein and Neuraminidase (NA) are the two main drug targets for commonly available drugs. M2 protein inhibitors like amantadine and rimantadine have narrow spectrum of activity, hence provide limited protection(Hay et al., 1985, Hastings et al., 1996, Mammen et al., 1995, Colman, 1989, De Clercq, 2001). Another target Neuraminidase (NA) is a glycoprotein. It acts as an enzyme and participates in the release of the progeny virus from infected cells(Gong et al., 2007, Varghese and Colman, 1991). Two well - known Neuraminidase inhibitors are Zanamivir and Oseltamivir. Zanamivir is known for excellent anti-viral activity during intranasal administration but is not too effective when delivered systemically. Oral bioavailability of Zanamivir is low and easily eliminated by renal excretion(Ryan et al., 1995). Oseltamivir is orally active but the associated side effects like vomiting, nausea and several allergic reactions do not augur well for a promising drug(Burch et al., 2009). Few other Neuraminidase inhibitors such as Peramivir, Laninamivir are in phase III clinical trials (Hata et al., 2014). Peramivir shows less oral bioavailability as compared to Oseltamivir(de Jong et al., 2014). So the situation is worrying and there is a need to design and identify new effective compounds for chemotherapy of influenza virus infection.

Pharmacophore modeling is one of the most important and extensively used method in ligand - based drug design. There are various studies in literature where pharmacophore modeling was used as an effective tool to understand the important features for well - known target inhibitors. The pharmacophore model is widely acknowledged as a balanced quantitative model that can be used to explore common chemical characteristics among a considerable number of structures with great diversity. Qualified pharmacophore model could also be used as a query for searching chemical databases to find new chemical entities. Quantitative Structure-Activity Relationship (QSAR) is an effective statistical method used to design new chemical moieties from the previous knowledge of activity of known compounds(John et al., 2010, Li et al., 2015). Different classes of inhibitors could be useful in digging out valuable information for developing new potent NA inhibitors.

This study aims to construct the chemical features based on pharmacophore models for neuraminidase. A high correlation quantitative pharmacophore model was generated, using observed structure-activity relationship of known neuraminidase inhibitors. The pharmacophore modeling was successfully applied for the development of new model and validated with available methods. This work is significant in connection with discovery of new molecules and may contribute to the development of more effective chemical moieties.

MATERIALS AND METHODS

(1) Selection of Data Set Compounds

3D QSAR method is one of the ligand – based pharmacophore modeling strategies used for the discovery of new effective compounds [12]. This strategy diverges from the usual pharmacophore approach in the number of training set compounds' requirement and need of experimental activity values predicted through similar bioassay conditions, etc. A data set of 46 compounds was retrieved from BRENDA database and literature and the redundancy was removed (Schomburg et al., 2004). Out of 46 compounds, 18 diverse compounds were selected for training data set with the experimental activity values (IC_{50}) ranging from 0.0032 nM to 8640 nM and structural diversity. These compounds were also utilized in pharmacophore cross - validation.

(2) Compound Preparation and Conformation Generation

The ChemSketch Version 12 was used to design the 2D structures of compounds and conversion of these compounds to 3D structures was done with the help of Accelrys Discovery Studio 3.1. Hydrogen atoms were then added to these prepared compounds and verified later. This was followed by energy minimization process using *Smart Minimizer* that carries out 1000 steps of steepest descent. This is then followed by application of conjugate gradient algorithms with convergence gradient of 0.001 kcal/mol. After completion of energy minimization, a number of acceptable conformers were generated for every training set compound within DS *Diverse conformation generation* module employing the poling algorithm for conformational analysis. The poling algorithm eliminates the chances of redundancy in conformation generation and this, in turn, improves the coverage of the conformational space. Within an energy range of 20kcal/mol above the global energy minimum, maximum number of conformers generated for each compound was limited to 255 (Schuster et al., 2006, Bharatham et al., 2007, Neves et al., 2009). This practically means that the difference in energy values among

different conformers of a particular compound was < 20kcal/mol.

(3) Generation of Pharmacophore Models

Ligand – based pharmacophore modeling is divided into two types methodologies one is common feature pharmacophore modeling utilized the common features present only in the most active compounds and another one based on 3D QSAR pharmacophore–the new design compounds activity estimated by using pharmacophore models, generation of this model by used the most active and inactive compounds' chemical features with pharmacological activity. The training set compounds features identify by feature mapping protocol available in DS. The values of Uncertainty and the minimum inter – feature distances were set respectively to 2 and 2Å. In DS -3D QSAR pharmacophore generation used the Feature mapping protocol identified hydrogen bond acceptor (HBA), hydrogen bond donor (HBD), hydrophobic aliphatic (HY-AL), hydrophobic aromatic (HY-AR) and ring aromatic (RA) features with other default values to generate ten pharmacophore models.

Biological activity of compounds that is directly relatively contributed to each feature of the model has a certain weight. The process of HypoGen pharmacophore model generation divided into three major steps - the constructive phase, the subtractive phase and the optimization phase(Kurogi and Guner, 2001, Kansal et al., 2010). In constructive phase of Hypotheses identified the common maximum number of active set compounds. HypoGen all combinations of pharmacophore features using for determines all possible pharmacophore configurations Apart from this, the hypotheses must fit a minimum subset of features of the remaining most active compounds. The end of the constructive phase coincides with generation of a large database of pharmacophore configurations. The subtractive phase, on the other hand, goes through elimination of all phramacophore configurations that also exist in the least active set of molecules. The least active molecules here are considered to be those compounds whose activity levels are less by 3.5 orders of magnitude than that of the most active compound, though this order is not fixed and can be modified in accordance with the activity of the training set.

The errors in activity estimates obtained through regression and complexity serve as adequate basis for scoring the hypotheses. The hypotheses scores get further improved in the optimization phase. This phase employs a simulated annealing approach. The activity prediction is optimized by considering variation of features and/or locations. HypoGen stops after reaching the point beyond which no further score improvement is possible. It then provides top scoring 10 unique pharmacophore models. The reliability of these models is assesses on the basis of different cost parameters. The overall cost of a model consists of the weight cost, the error cost, and the configuration cost. The weight cost shows a Gaussian increase pattern, the error cost is an indication of the difference between estimated and measured activities of the training set and the configuration cost is a quantitative measure of the hypothesis space entropy.

The generation of pharmacophore models also involves calculation of three additional cost values – the fixed cost, the total cost, and the null cost. The fixed cost is the least possible cost that represents the simplest hypothetical model that provides a perfect fit for the data. Fixed costs consist of minimum achievable error, weight cost and the constant configuration cost. The null cost, on the other hand, is the maximum cost of a pharmacophore and calculates the average of activity data of training set molecules. It matches with the maximum error cost. To generate a pharmacophore model, a total of ten cost values along with their fixed and null cost were estimated. Ideally, the model should have a low fixed cost and high null cost values. Alongside, the difference between the total and fixed values should be minimum whereas the difference between total and null values should be maximum (Sundarapandian et al., 2010, Sanam et al., 2009). Further, regression analysis was performed employing HypoGen for predicting activity of the training set compounds. This study was done using the relationship of geometric fit value V/s the negative logarithm of activity. The activity prediction is directly proportional to the geometric fitness. Other statistical parameters, namely - correlation coefficient and root mean square deviation (RMSD) were also computed. Finally, the model with high cost difference and correlation coefficient with low RMSD was selected.

(4) Pharmacophore Cross Validation

The models were cross validated to assess their ability to predict the activity of any new compound. The identified best model was validated via two approaches based on derived cost modules - the Fischer randomization test and leave – one - out method. All the cost values are stated in bits and 75 - 90% correlation is proposed by a difference of 40 - 60 bits. The Fischer randomization approach for validation of the pharmacophore model involved construction of 19 random spread sheets with 95% confidence level (Sarma et al., 2008, Thangapandian et al., 2011a). In this study the correlation between the biological activity and the chemical structures is tested by randomizing the activity data of training set compounds. The models were generated using the same parameters which were used to build the original model but the activity values were randomized. The second is the leave – one - out method, where 18 pharmacophore models were generated with the same parameters used for generating original

pharmacophore model but leaving one compound at a time from the training set compounds. This is done to state the effect of every single training set compound in the generation of selected pharmacophore model (Stoll et al., 2002, Zampieri et al., 2009).

RESULT AND DISCUSSION

PHARMACOPHORE GENERATION

A training set with 18 compounds is used for the generation of ten pharmacophore models. Structures of these training set compounds are shown in **(Figure 1).** These models were generated by using HBA, HBD, HY-AL, HY-AR and RA features from the *Feature Mapping Protocol(*Arooj et al., 2013). All the selected pharmacophore models consisted of either HBA or HBD or both, with HY-AL or HY-AR. Total cost values ranged from 94.22 to 98.28.

The pharmacophore generation run in this study revealed fixed cost value and null cost value as 77.44 and 157.052 respectively. The analysis of ten generated pharmacophores models indicates that the total cost value for the first model (Hypo 1) is the closest to the fixed cost value vis – à - vis other models. The cost difference between the null cost and total cost value of the first pharmacophore model is 62.83 **(Table 1).** A cost difference value between 40 and 60 signifies that the pharmacophore model correlates the experimental and predicted activity. Herein, the cost difference value of Hypo 1 signifies the correlation between the experimental and predicted activity values of more than 90% of the training set compounds(Vuorinen et al., 2014, Kandakatla and Ramakrishnan, 2014). The Hypo 1 pharmacophore model, being the best, was selected and consisted of two HBA, one HBD and one HY-AL features **(Figure 2).**

Further investigation of the generated pharmacophore models was based on the selected ten pharmacoph-

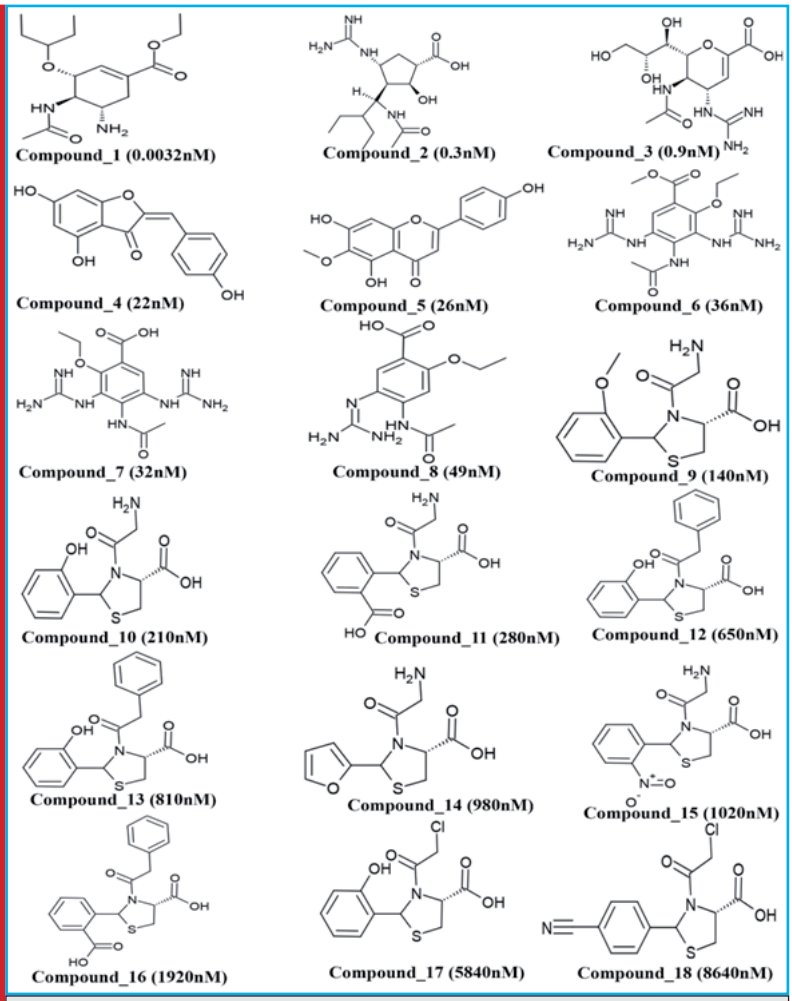

FIGURE 1. 2D Structure of the training set compounds. 2D Chemical structures of the 18 training set with their experimental IC50 values

Table 1. Statistical Results of the 10 Pharmacophore Hypothesis generated by Hypo Gen Algorithm

Hypothesis	Total cost	Cost difference	RMSD	Correlation	Features
Hypo 1	94.2211	62.8309	1.30795	0.917666	HBA HBD HBD HY-AL
Hypo 2	95.2269	61.8251	1.36582	0.909478	HBA HBD HBD HY-AL
Hypo 3	96.7312	60.3208	1.40736	0.903947	HBA HBD HBD HY-AL
Hypo 4	97.0164	60.0356	1.41827	0.902366	HBA HBD HBD HY-AL
Hypo 5	97.34	59.712	1.44001	0.898952	HBA HBD HBD HY-AL
Hypo 6	97.9418	59.1102	1.50229	0.888384	HBA HBD HBD HY-AL
Hypo 7	98.251	58.801	1.50229	0.888384	HBA HBD HBD HY-AL
Hypo 8	98.2555	58.7965	1.50857	0.887742	HBA HBD HBD HY-AL
Hypo 9	98.2683	58.7837	1.5014	0.889011	HBA HBD HBD HY-AL
Hypo 10	98.2848	58.7672	1.49708	0.889783	HBA HBD HBD HY-AL

Null cost = 157.052; fixed cost = 77.44; configuration cost = 15.77
Cost difference = null cost – total cost.
HBA, hydrogen bond acceptor; HBD, hydrogen bond donor; hydrophobic aliphatic

ore models having correlation values greater than 0.889. Out of them, the top four pharmacophore models correlated the activity data with high correlation values that were higher than 0.9. These results indicate the capability of the pharmacophore model to predict the activity of the training set compounds. Hypo 1 showed the highest correlation coefficient value of 0.9, thus highlighting its strong predictive ability (Muthusamy et al., 2015). RMSD values calculated for the top five pharmacophore models were less than 1.5 which supports our find-

Table 2. Experimental and Estimated IC_{50} Values of the Training Set Compounds based on Best Pharmacophore.

Name	IC_{50} nM		Error	Fit value	Activity scale	
	Experimental	Estimated			Experimental	Estimated
Compound 1	0.0032	0.012	2.6	9.65	++++	++++
Compound 2	0.3	0.34	3.9	8.21	++++	++++
Compound 3	0.9	3.7	2.8	7.17	++++	++++
Compound 4	22	850	21	4.81	+++	++
Compound 5	26	170	13	5.52	+++	+++
Compound 6	36	12	-4.1	6.68	+++	+++
Compound 7	32	56	-1.3	5.99	+++	+++
Compound 8	49	66	-1.3	5.92	+++	+++
Compound 9	140	19	-7.6	6.45	+++	+++
Compound 10	210	38	6.16	1.1	++	+++
Compound 11	280	240	1.1	5.36	++	++
Compound 12	650	750	-1.6	4.86	++	++
Compound 13	810	550	-1.8	5	++	++
Compound 14	980	620	-2.2	4.95	++	++
Compound 15	1020	560	-2.8	4.99	+	++
Compound 16	1920	5300	5.9	4.01	+	+
Compound 17	5840	730	-15	4.87	+	++
Compound 18	8640	1800	-3.9	4.48	+	+

[a]Positive value indicates that the estimate IC_{50} is higher than the experimental IC_{50}; negative value indicates that the estimate IC_{50} is lower than the experimental IC_{50}.
[b]Fit value indicates how well the features in the pharmacophore map the chemical features in the compound
Activity scale: $IC_{50} \leq 10$ nM (Most active, ++++); $10 < IC_{50} \leq 200$ nM (Active, +++); $200 < IC_{50} \leq 1000$ nM (Moderately active, ++); > 1000 nM
(inactive, +)

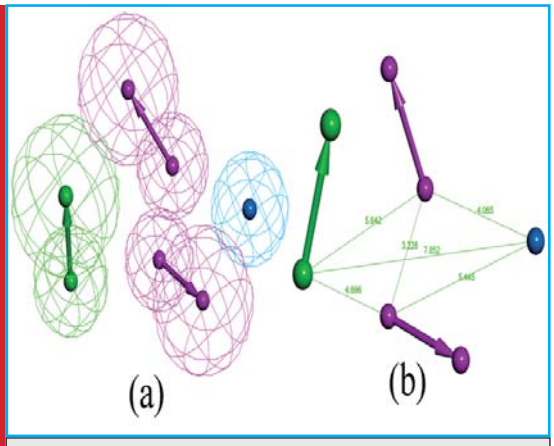

FIGURE 2. The Best HypoGen Pharmacophore Model, Hypo 1. (a) Chemical features present in Hypo 1 (b) 3D Spatial Arrangement and the Distance Constraints between the Chemical Features. Green color represents HBA, magenta color represents HBD and cyan color represents HY-AL.

ings (Niu et al., 2014). Hypo 1 was developed with better statistical values, such as higher correlation, large cost difference, and low RMSD (1.30795). Hypo 1 has predicted the experimental activity values of training set compounds with high correlation. All compounds in the training set were categorized into four different groups based on their experimental activity (IC_{50}) values: most active ($IC_{50} \leq 10$ nM, ++++), active ($10 < IC_{50} \leq 200$ nM, +++), moderately active ($200 < IC_{50} \leq 1000$ nM, ++), and inactive ($IC_{50} > 1000$ nM, +).

The predictive ability of Hypo 1 on training set compounds is shown in **(Table 2).** In accordance with the Hypo1 activity values, 15 out of 18 compounds in the training set were predicted within their experimental activity scale whereas compounds 10, 15, and 17 were over estimated as active. None of the calculated error values representing the ratio between the experimental and predicted activity values were more than one order of magnitude. All of the three most active compounds in the training set were predicted very close to their activity values indicating the predictive ability of Hypo 1. The most active compounds in training set mapped all the features of Hypo 1 whereas the other compounds missed at least one of the pharmacophoric features.

The pharmacophore mapping of the most active and the least active compounds is shown in **(Figure 3).** Among top four hypotheses, Hypo 1 is the best model over others which have also shown a high correlation value (0.91) with HBA, HBD and HY-AL features (Thangapandian et al., 2011b). The energy values of the conformations of the most active compounds in the training set used in model generation were lower in Hypo 1 but relatively higher in Hypo 2. This analysis also supported the reliability of Hypo 1 along with the high correlation coefficient.

PHARMACOPHORE CROSS VALIDATION

(a) Fisher Randomization Test

The Fisher randomization test used for testifying and validating Hypo 1 indicates that this pharmacophore model does not occur due to the random correlation (Singh and Singh, 2013). The experimental activities of the training set were picked randomly and the resulting

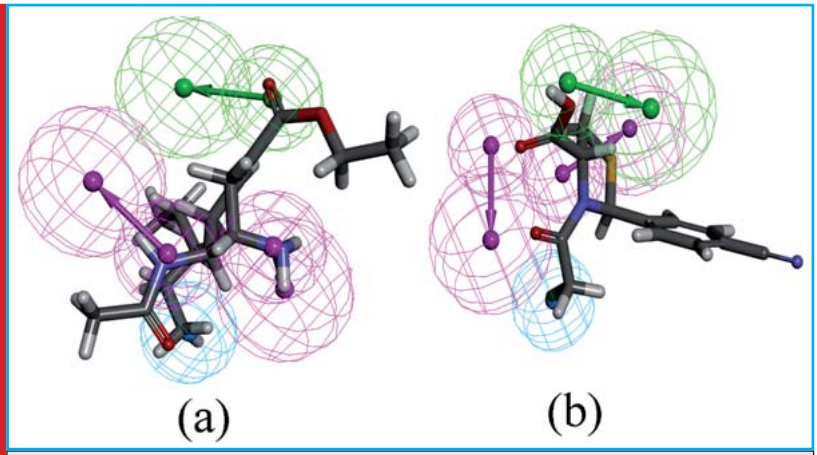

FIGURE 3. Pharmacophore Mapping: Mapping of the most active compounds 1, IC50 = 0.0032 mapped on the best pharmacophore model; (b) the least active compound (compound 18, IC50 = 8640) mapped on the best pharmacophore model (Hypo 1). In the pharmacophore model - green represents HBA, magenta represents HBD and cyan represents HY-AL features.

Table 3. Fisher Randomization test results.

Validation no	Total cost	Null cost	Cost Diff.	correlation
Original hypothesis				
Hypo 1	94.22	157.052	62.83	0.917666
Randomized hypothesis				
Trail 1	103.517	157.052	53.535	0.871634
Trail 2	109.558	157.052	47.494	0.854541
Trail 3	108.675	157.052	48.377	0.84838
Trail 4	107.26	157.052	49.792	0.860989
Trail 5	108.599	157.052	48.453	0.856582
Trail 6	132.103	157.052	24.949	0.655598
Trail 7	115.443	157.052	41.609	0.805429
Trail 8	112.835	157.052	44.217	0.804367
Trail 9	122.52	157.052	34.532	0.724558
Trail 10	112.816	157.052	44.236	0.885913
Trail 11	113.451	157.052	43.601	0.801793
Trail 12	115.03	157.052	42.022	0.868995
Trail 13	101.264	157.052	55.788	0.89344
Trail 14	105.574	157.052	51.478	0.919629
Trail 15	115.66	157.052	41.392	0.784862
Trail 16	110.194	157.052	46.858	0.906808
Trail 17	114.316	157.052	42.736	0.779937
Trail 18	127.639	157.052	29.413	0.780038
Trail 19	127.029	157.052	24.95	0.692584

training set was used in HypoGen with the parameters chosen for the original pharmacophore generation. A set of 19 random spread sheets was generated to achieve a 95% confidence level that the best pharmacophore Hypo 1 was not generated by chance (Sakkiah and Lee, 2012) shown in **(Table 3)**. None of the randomly generated pharmacophore models during Fisher randomization test has scored better statistical parameters than Hypo 1. Though four random pharmacophores scored a correlation value higher than 0.9 (i. e. than Hypo 1).

(b) Leave – one – out method

Leave – one - out method was used for final validation(Niu et al., 2013). This method is used to verify if the correlation between the experimental and predicted activities is primarily dependent on one particular molecule in the training set, or otherwise. This is done by applying recursive iteration on the pharmacophore model by excluding one molecule in every iteration cycle. The 18 HypoGen calculations were carried out under conditions that were identical to the ones used in the generation of original pharmacophore model Hypo 1. 18 new training sets, each containing 17 molecules, were derived. The correlation coefficients of newly generated pharmacophore models were computed. A positive result emerges if none of the correlation coefficients of newly generated pharmacophore models is higher or too lower to that of Hypo 1. The findings establish that none of the 18 new models generated by this method has any significant difference vis – a - vis Hypo 1. This result enhances the confidence level of Hypo 1regarding the non – dependence of correlation coefficient on any particular compound in the training set.

CONCLUSION

The present study is an attempt to generate a quantitative pharmacophore model for neuraminidase enzyme by employing a dataset of known inhibitors. A model (Hypo 1) was developed based on the training set compounds with high chemical structure diversity and significant divergence in biological activity values (IC_{50}). The best pharmacophore model was selected on the basis of various parameters like cost difference, correlation co – efficient, and the validation results. All these validation procedures have shown and confirmed the strength of the selected model Hypo 1. These validation results

throw interesting opportunities for further database screening to identify the small molecule which can be used in neuraminidase inhibitor design and may provide leads in the world's fight against *Influenza A Virus*.

ACKNOWLEDGEMENT

The authors are thankful to Maulana Azad National Institute of Technology (MANIT), Bhopal, and MHRD, GOI, for providing financial assistance. Special thanks are due to Dr. Ajay Pandey, a faculty member at MANIT, Bhopal, for his valuable support, help, and guidance during the preparation of this manuscript.

CONFLICT OF INTEREST

The authors declare that they have no conflict of interest.

REFERENCES

Arooj, M., Sakkiah, S., Kim, S., Arulalapperumal, V. and Lee, K. W. (2013): A combination of receptor-based pharmacophore modeling & QM techniques for identification of human chymase inhibitors. PLoS One, 8(4), pp. e63030.

Bharatham, N., Bharatham, K. and Lee, K. W. (2007): Pharmacophore identification and virtual screening for methionyl-tRNA synthetase inhibitors. Journal of Molecular Graphics and Modelling, 25(6), pp. 813-823.

Burch, J., Corbett, M., Stock, C., Nicholson, K., Elliot, A. J., Duffy, S., Westwood, M., Palmer, S. and Stewart, L. (2009): Prescription of anti-influenza drugs for healthy adults: a systematic review and meta-analysis. The Lancet infectious diseases, 9(9), pp. 537-545.

Colman, P. M. (1989): 'Neuraminidase', The influenza viruses. Springer, pp. 175-218.

De Clercq, E. (2001): Antiviral drugs: current state of the art. Journal of Clinical Virology, 22(1), pp. 73-89.

de Jong, M. D., Ison, M. G., Monto, A. S., Metev, H., Clark, C., O'neil, B., Elder, J., McCullough, A., Collis, P. and Sheridan, W. P. (2014): Evaluation of intravenous peramivir for treatment of influenza in hospitalized patients. Clinical Infectious Diseases, 59(12), pp. e172-e185.

Ducatez, M. F., Pelletier, C. and Meyer, G. (2015): Influenza D virus in cattle, France, 2011–2014. Emerging infectious diseases, 21(2), pp. 368.

Ferguson, L., Eckard, L., Epperson, W. B., Long, L.-P., Smith, D., Huston, C., Genova, S., Webby, R. and Wan, X.-F. (2015): Influenza D virus infection in Mississippi beef cattle. Virology, 486, pp. 28-34.

Gong, J., Xu, W. and Zhang, J. (2007): Structure and functions of influenza virus neuraminidase. Current medicinal chemistry, 14(1), pp. 113-122.

Hastings, J., Selnick, H., Wolanski, B. and Tomassini, J. (1996): Anti-influenza virus activities of 4-substituted 2, 4-dioxobutanoic acid inhibitors. Antimicrobial agents and chemotherapy, 40(5), pp. 1304-1307.

Hata, A., Akashi-Ueda, R., Takamatsu, K. and Matsumura, T. (2014): Safety and efficacy of peramivir for influenza treatment. Drug design, development and therapy, 8, pp. 2017.

Hay, A., Wolstenholme, A., Skehel, J. and Smith, M. H. (1985): The molecular basis of the specific anti-influenza action of amantadine. The EMBO journal, 4(11), pp. 3021.

John, S., Thangapandian, S., Sakkiah, S. and Lee, K. W. (2010): Identification of potent virtual leads to design novel indoleamine 2, 3-dioxygenase inhibitors: Pharmacophore modeling and molecular docking studies. European journal of medicinal chemistry, 45(9), pp. 4004-4012.

Kandakatla, N. and Ramakrishnan, G. (2014): Ligand based pharmacophore modeling and virtual screening studies to design novel HDAC2 inhibitors. Advances in bioinformatics, 2014.

Kansal, N., Silakari, O. and Ravikumar, M. (2010): Three dimensional pharmacophore modelling for c-Kit receptor tyrosine kinase inhibitors. European journal of medicinal chemistry, 45(1), pp. 393-404.

Kobasa, D., Takada, A., Shinya, K., Hatta, M., Halfmann, P., Theriault, S., Suzuki, H., Nishimura, H., Mitamura, K. and Sugaya, N. (2004): Enhanced virulence of influenza A viruses with the haemagglutinin of the 1918 pandemic virus. Nature, 431(7009), pp. 703-707.

Kurogi, Y. and Guner, O. F. (2001): Pharmacophore modeling and three-dimensional database searching for drug design using catalyst. Current medicinal chemistry, 8(9), pp. 1035-1055.

Li, C., Fang, J. S., Lian, W. W., Pang, X. C., Liu, A. L. and Du, G. H. (2015): In vitro antiviral effects and 3D QSAR study of resveratrol derivatives as potent inhibitors of influenza H1N1 neuraminidase. Chemical biology & drug design, 85(4), pp. 427-438.

Mammen, M., Dahmann, G. and Whitesides, G. M. (1995): Effective inhibitors of hemagglutination by influenza virus synthesized from polymers having active ester groups. Insight into mechanism of inhibition. Journal of medicinal chemistry, 38(21), pp. 4179-4190.

Muthusamy, K., Kirubakaran, P., Krishnasamy, G. and Thanashankar, R. R. (2015): Computational Insights into the Inhibition of Influenza Viruses by Rupestonic Acid Derivatives: Pharmacophore Modeling, 3D-QSAR, CoMFA and COMSIA Studies. Combinatorial chemistry & high throughput screening, 18(1), pp. 63-74.

Nayak, B., Kumar, S., DiNapoli, J. M., Paldurai, A., Perez, D. R., Collins, P. L. and Samal, S. K. (2010): Contributions of the avian influenza virus HA, NA, and M2 surface proteins to the induction of neutralizing antibodies and protective immunity. Journal of virology, 84(5), pp. 2408-2420.

Neves, M. A., Dinis, T. C., Colombo, G. and e Melo, M. L. S. (2009): An efficient steroid pharmacophore-based strategy to

identify new aromatase inhibitors. European journal of medicinal chemistry, 44(10), pp. 4121-4127.

Niu, M.-m., Qin, J.-y., Tian, C.-p., Yan, X.-f., Dong, F.-g., Cheng, Z.-q., Fida, G., Yang, M., Chen, H. and Gu, Y.-q. (2014): Tubulin inhibitors: pharmacophore modeling, virtual screening and molecular docking. Acta Pharmacologica Sinica, 35(7), pp. 967-979.

Niu, M., Dong, F., Tang, S., Fida, G., Qin, J., Qiu, J., Liu, K., Gao, W. and Gu, Y. (2013): Pharmacophore modeling and virtual screening for the discovery of new type 4 cAMP phosphodiesterase (PDE4) inhibitors. PloS one, 8(12), pp. e82360.

Rajao, D. S. and Vincent, A. L. (2015): Swine as a model for influenza a virus infection and immunity. ILAR Journal, 56(1), pp. 44-52.

Renzette, N., Caffrey, D. R., Zeldovich, K. B., Liu, P., Gallagher, G. R., Aiello, D., Porter, A. J., Kurt-Jones, E. A., Bolon, D. N. and Poh, Y.-P. (2014): Evolution of the influenza A virus genome during development of oseltamivir resistance in vitro. Journal of virology, 88(1), pp. 272-281.

Ryan, D. M., Ticehurst, J. and Dempsey, M. H. (1995): GG167 (4-guanidino-2, 4-dideoxy-2, 3-dehydro-N-acetylneuraminic acid) is a potent inhibitor of influenza virus in ferrets. Antimicrobial agents and chemotherapy, 39(11), pp. 2583-2584.

Sakkiah, S. and Lee, K. W. (2012): Pharmacophore-based virtual screening and density functional theory approach to identifying novel butyrylcholinesterase inhibitors. Acta Pharmacologica Sinica, 33(7), pp. 964-978.

Sanam, R., Vadivelan, S., Tajne, S., Narasu, L., Rambabu, G. and Jagarlapudi, S. A. (2009): Discovery of potential ZAP-70 kinase inhibitors: Pharmacophore design, database screening and docking studies. European journal of medicinal chemistry, 44(12), pp. 4793-4800.

Sarma, R., Sinha, S., Ravikumar, M., Kumar, M. K. and Mahmood, S. (2008): Pharmacophore modeling of diverse classes of p38 MAP kinase inhibitors. European journal of medicinal chemistry, 43(12), pp. 2870-2876.

Schomburg, I., Chang, A., Ebeling, C., Gremse, M., Heldt, C., Huhn, G. and Schomburg, D. (2004): BRENDA, the enzyme database: updates and major new developments. Nucleic acids research, 32(suppl 1), pp. D431-D433.

Schuster, D., Laggner, C., Steindl, T. M., Palusczak, A., Hartmann, R. W. and Langer, T. (2006): Pharmacophore modeling and in silico screening for new P450 19 (aromatase) inhibitors. Journal of chemical information and modeling, 46(3), pp. 1301-1311.

Singh, A. and Singh, R. (2013): QSAR and its role in target-ligand interaction. Open Bioinformatics Journal, 7, pp. 63-67.

Stoll, F., Liesener, S., Hohlfeld, T., Schrör, K., Fuchs, P. L. and Höltje, H.-D. (2002): Pharmacophore definition and three-dimensional quantitative structure-activity relationship study on structurally diverse prostacyclin receptor agonists. Molecular pharmacology, 62(5), pp. 1103-1111.

Sundarapandian, T., Shalini, J., Sugunadevi, S. and Woo, L. K. (2010): Docking-enabled pharmacophore model for histone deacetylase 8 inhibitors and its application in anti-cancer drug discovery. Journal of Molecular Graphics and Modelling, 29(3), pp. 382-395.

Thangapandian, S., John, S., Sakkiah, S. and Lee, K. W. (2011a): Pharmacophore-based virtual screening and Bayesian model for the identification of potential human leukotriene A4 hydrolase inhibitors. European journal of medicinal chemistry, 46(5), pp. 1593-1603.

Thangapandian, S., John, S., Sakkiah, S. and Lee, K. W. (2011b): Potential virtual lead identification in the discovery of renin inhibitors: Application of ligand and structure-based pharmacophore modeling approaches. European journal of medicinal chemistry, 46(6), pp. 2469-2476.

Varghese, J. and Colman, P. M. (1991): Three-dimensional structure of the neuraminidase of influenza virus A/Tokyo/3/67 at 2· 2 Å resolution. Journal of molecular biology, 221(2), pp. 473-486.

Vuorinen, A., Engeli, R., Meyer, A., Bachmann, F., Griesser, U. J., Schuster, D. and Odermatt, A. (2014): Ligand-based pharmacophore modeling and virtual screening for the discovery of novel 17β-hydroxysteroid dehydrogenase 2 inhibitors. Journal of medicinal chemistry, 57(14), pp. 5995-6007.

Zampieri, D., Mamolo, M. G., Laurini, E., Florio, C., Zanette, C., Fermeglia, M., Posocco, P., Paneni, M. S., Pricl, S. and Vio, L. (2009): Synthesis, biological evaluation, and three-dimensional in silico pharmacophore model for σ1 receptor ligands based on a series of substituted benzo [d] oxazol-2 (3 H)-one derivatives. Journal of medicinal chemistry, 52(17), pp. 5380-5393.